








Cladistical Analysis of the Jovian and Saturnian Satellite Systems

Timothy. R. Holt^{1,2} , Adrian. J. Brown³ , David Nesvorný⁴ , Jonathan Horner¹ , and Brad Carter¹ 
¹ University of Southern Queensland, Computational Engineering and Science Research Centre, Queensland, Australia; timothy.holt@usq.edu.au
² Swinburne University of Technology, Center for Astrophysics and Supercomputing, Victoria, Australia
³ Plancius Research LLC, Severna Park, MD, USA
⁴ Southwest Research Institute, Department of Space Studies, Boulder, CO, USA

Received 2017 June 4; revised 2018 April 9; accepted 2018 April 10; published 2018 May 29

Abstract

Jupiter and Saturn each have complex systems of satellites and rings. These satellites can be classified into dynamical groups, implying similar formation scenarios. Recently, a larger number of additional irregular satellites have been discovered around both gas giants that have yet to be classified. The aim of this paper is to examine the relationships between the satellites and rings of the gas giants, using an analytical technique called *cladistics*. Cladistics is traditionally used to examine relationships between living organisms, the “tree of life.” In this work, we perform the first cladistical study of objects in a planetary science context. Our method uses the orbital, physical, and compositional characteristics of satellites to classify the objects in the Jovian and Saturnian systems. We find that the major relationships between the satellites in the two systems, such as families, as presented in previous studies, are broadly preserved. In addition, based on our analysis of the Jovian system, we identify a new retrograde irregular family, the Iocaste family, and suggest that the Phoebe family of the Saturnian system can be further divided into two subfamilies. We also propose that the Saturnian irregular families be renamed, to be consistent with the convention used in Jovian families. Using cladistics, we are also able to assign the new unclassified irregular satellites into families. Taken together, the results of this study demonstrate the potential use of the cladistical technique in the investigation of relationships between orbital bodies.

Key words: methods: data analysis – planets and satellites: composition – planets and satellites: formation – planets and satellites: general

Supporting material: machine-readable tables

1. Introduction

The two gas giants of the Solar system, Jupiter and Saturn, are host to a large number of satellites and rings. The satellites of both planets follow a similar progression pattern. The inner region of each system consists of small icy satellites, with an accompanying ring system (Thomas et al. 1998, 2013; Throop et al. 2004; Porco et al. 2005). Further out, there are larger icy/silicate satellites (Thomas 2010; Deienno et al. 2014). In the outer system, both planets have a series of irregular satellites, small satellites with high eccentricities and inclinations (Nesvorný et al. 2003; Sheppard & Jewitt 2003; Jewitt & Haghighipour 2007). It is thought that these satellites were captured from other populations of small Solar system bodies (Colombo & Franklin 1971; Heppenheimer & Porco 1977; Pollack et al. 1979; Sheppard & Jewitt 2003; Nesvorný et al. 2004, 2007, 2014; Johnson & Lunine 2005). This is in contrast to the inner satellites, which are thought to have accreted in a circumplanetary disk (e.g., Canup & Ward 2002; Canup 2010). Such a formation mechanism is thought to resemble the accretion of planets in a protoplanetary disk around a young star (Lissauer 1987), a conclusion that is supported by the recent discovery of the TRAPPIST-1 planetary system (Gillon et al. 2016). That system features at least seven Earth-mass planets orbiting a very low mass star. The star itself, TRAPPIST-1, is within two orders of magnitude more massive than Jupiter, and similar in size. The seven planets span an area comparable to that of Jupiter’s regular satellite system. Studying and understanding the gas giant systems in our own Solar system can therefore provide context for future exploration of low mass exoplanetary systems.

1.1. The Jovian System

Historically, Galilei (1610) discovered the first satellites in the Jovian system, the large Galileans, Io, Europa, Ganymede, and Callisto. Our knowledge of these satellites has increased greatly, as a result of both improved ground-based instrumentation (e.g., Sparks et al. 2016; Vasundhara et al. 2017) and spacecraft visitations (e.g., Smith et al. 1979; Grundy et al. 2007; Greenberg 2010).

Amalthea, one of the inner set of Jovian satellites, was discovered by Barnard (1892). A few years later, the first two small irregular satellites, Himalia (Perrine 1905) and Elara (Perrine & Aitken 1905), were discovered in inclined, prograde orbits. The discovery of Pasiphae 3 years later by Melotte & Perrine (1908) is significant, as this was only the second satellite in the Solar system to be found on a retrograde orbit, and the first such object found in the Jovian system. Several other irregular satellites were discovered in the first half of the 20th century: Sinope (Nicholson 1914), Lysithea (Nicholson 1938), Carme (Nicholson 1938), and Ananke (Nicholson 1951). Leda, another small prograde irregular, was discovered 20 years later by Kowal et al. (1975b). Themisto, the first Jovian satellite smaller than 10 km to be discovered, was found that same year (Kowal et al. 1975a) and subsequently lost. Themisto was rediscovered by Sheppard et al. (2000) nearly 20 years later. The *Voyager* visitations of Jupiter discovered the remaining three inner satellites, Metis (Synnott 1981), Adrastea (Jewitt et al. 1979), and Thebe (Synnott 1980), along with a ring system (Smith et al. 1979). These three satellites, Amalthea, and the ring system would be imaged again by the

Galileo (Ockert-Bell et al. 1999) and *Cassini* (Porco et al. 2005) spacecraft during their missions.

The irregular Jovian satellites orbit the planet with semimajor axes an order of magnitude greater than the Galilean moons, and have large eccentricities and inclinations. In the early years of the 21st century, extensive surveys were carried out to search for the Jovian irregular satellites (Scotti et al. 2000; Sheppard et al. 2001, 2002, 2003b, 2004; Gladman et al. 2003a, 2003b; Sheppard & Jewitt 2003; Sheppard & Marsden 2003a, 2003b, 2004; Beaugé & Nesvorný 2007; Jacobson et al. 2011; Sheppard & Williams 2012). These surveys increased the number of known Jovian satellites from 14 after *Voyager* to the 67 known today. The inner five irregular satellites, Leda, Himalia, Lystea, Elara and Dia, have prograde orbits and have previously been classified into the Himalia group (Nesvorný et al. 2003; Sheppard & Jewitt 2003). Themisto and Carpo were proposed as single members of their own groups by Sheppard & Jewitt (2003). The remainder of the irregular satellites have retrograde orbits. Based on similarities in semimajor axis, inclination, and eccentricity, these satellites have been grouped into families by Sheppard & Jewitt (2003) and Nesvorný et al. (2003). These dynamical families are typified by their largest member, Himalia, representing the inner prograde satellites, with the retrograde ones being broken down into the Ananke, Pasiphae, and Carme families. Recently, several additional small irregular satellites have been discovered (Jacobson et al. 2011; Sheppard & Williams 2012), which are yet to be named or classified. With the discovery of new satellites (Scotti et al. 2000; Sheppard et al. 2001; Beaugé & Nesvorný 2007; Jacobson et al. 2011; Sheppard & Williams 2012) and additional information from the *Cassini* spacecraft (Porco et al. 2005), a revisit of the classification of the Jovian irregular satellites (Nesvorný et al. 2003; Sheppard & Jewitt 2003; Jewitt & Haghhighipour 2007) is warranted.

1.2. The Saturnian System

The Saturnian system is broadly similar to that of Jupiter, but exhibits greater complexity. One of the most striking features, visible to even the most modest telescope, is Saturn's ring system. First observed by Galileo in 1610, it was Huygens (1659) that observed that the objects surrounding Saturn were in fact rings. The rings themselves are composed of individual particles, from micrometer to meter size (Zebker et al. 1985). Embedded within several of the main rings are a series of small moonlets (Tiscareno et al. 2006) and several shepherd satellites (Showalter 1991; Porco et al. 2007; Cuzzi et al. 2014). The orbitals Janus and Epimetheus (Yoder et al. 1983, 1989; Nicholson et al. 1992; Treffenstädt et al. 2015; El Moutamid et al. 2016), and their associated faint ring system (Winter et al. 2016) are unique to the Saturn system. Just beyond the Janus/Epimetheus orbit, there is a diffuse G-ring, the source of which is the satellite Aegaeon (Hedman et al. 2007b).

Huygens (1659) also discovered Saturn's largest satellite, Titan. Earth-based observations highlighted the methane based atmosphere of Titan (Kuiper 1944; Karkoschka 1994), with further characterization by the *Cassini* spacecraft (Niemann et al. 2005) and Huygens lander (Lebreton et al. 2005). The bulk composition of Titan is analogous to that of the other icy satellites, with an icy shell, subsurface water ocean, and silicate core (Hemingway et al. 2013). There are seven other mid-sized icy satellites, with semimajor axes on a similar order of magnitude to that of Titan. The five largest, Mimas, Enceladus,

Tethys, Dione, and Rhea, are large enough to be in hydrostatic equilibrium. All of the mid-sized satellites are thought to be predominantly composed of water ice, with some contribution from silicate rock, and may contain subsurface liquid oceans (Matson et al. 2009; Filacchione et al. 2012). Those satellites closer to Saturn than Titan, Mimas, Enceladus, Tethys, Dione, and Rhea are embedded in the E-ring (Feibelman 1967; Baum et al. 1981; Hillier et al. 2007; Hedman et al. 2012). The *Cassini* mission identified the source of this ring as the southern cryo-plumes of Enceladus (Spahn et al. 2006).

In addition to the larger icy satellites, there are four small Trojan satellites (Porco et al. 2005), situated at the leading and trailing Lagrange points, 60° ahead or behind the parent satellites in their orbit. Tethys has Telesto and Calypso as Trojan satellites, while Helene and Polydeuces are Trojan satellites of Dione. So far, these Trojan satellites are unique to the Saturnian system. Between the orbits of Mimas and Enceladus, there are the Alkyonides, Methone, Anthe, and Pallene, recently discovered by the *Cassini* spacecraft (Porco et al. 2005). All of the Alkyonides have their own faint ring arcs (Hedman et al. 2009) composed of similar material to the satellite. Dynamical modeling by Sun et al. (2017) supports the theory of Hedman et al. (2009) that the parent satellite is the source of the rings.

In the outer Saturnian system there are a large number of smaller irregular satellites, with 38 known to date. The first of these irregular satellites to be discovered was Phoebe, which was the first planetary satellite to be discovered photographically (Pickering 1899). Phoebe was also the first satellite to be discovered moving on a retrograde orbit (Pickering 1905; Ross 1905). Phoebe is the best studied irregular satellite and the only one for which in situ observations have been obtained (Clark et al. 2005). Recently, a large outer ring associated with Phoebe and the other irregular satellites has been discovered (Verbiscer et al. 2009). It has been suggested that Phoebe may have originated in the Edgeworth–Kuiper Belt and captured into orbit around Saturn (Johnson & Lunine 2005). The other Saturnian irregular satellites were discovered in extensive surveys during the early 21st century (Gladman et al. 2001; Sheppard et al. 2003a, 2006b, 2007; Jewitt et al. 2005). Due to the small size of the majority of these satellites, only their orbital information is available. There are 9 prograde and 29 retrograde outer satellites, of which attempts have been made to place into families based on dynamical (Gladman et al. 2001; Jewitt & Haghhighipour 2007; Turrini et al. 2008) and photometric (Grav et al. 2003; Grav & Bauer 2007) information. In the traditional naming convention (Grav et al. 2003), the Inuit family, Ijiraq, Kiviuq, Paaliaq, Siarnaq, and Tarqeq are small prograde satellites, whose inclination is between 45° and 50° . The Gallic family, Albiorix, Bebhionn, Erriapus, and Tarvos, is a similar, prograde group, but with inclinations between 35° and 40° . The retrograde satellites are all grouped into the Norse family, including Phoebe. There is a possibility that the Norse family could be further split into subfamilies, based on photometric studies (Grav et al. 2003; Grav & Bauer 2007). The convention of using names from respective mythologies for the satellite clusters (Jewitt & Haghhighipour 2007) has become the default standard for the irregular satellite families of Saturn.

1.3. Formation Theories

The purpose of taxonomy and classification, beyond simple grouping, is to investigate the origin of objects. The origin of the irregular satellites is a major topic of ongoing study (Nesvorný & Morbidelli 2012; Nesvorný et al. 2014). Here we present an overview for context. There are three main theories in the formation of the Jovian satellites: formation via disk accretion (Canup & Ward 2002), via nebula drag (Pollack et al. 1979), or via dynamic capture (Nesvorný et al. 2003, 2007). The satellites that are captured, either by nebula drag or through dynamical means, are thought to be from Solar system debris, such as asteroids and comets.

The disk accretion theory has generally been accepted as the mechanism for the formation of the inner prograde satellites of Jupiter (Canup & Ward 2002). The satellites form from dust surrounding proto-Jupiter in a process analogous to the formation of planets around a star (Lissauer 1987). This surrounding disk would have lain in the equatorial plane of Jupiter, with material being accreted to the planet itself through the disk. This would explain both the prograde, coplanar orbits of the regular satellites and their near circular orbits.

The second theory requires satellites to be captured in the original Jovian nebula (Pollack et al. 1979; Ćuk & Burns 2004). Before it coalesced into a planet, Jupiter is proposed to have had a greater radius, and lower density than now. There was a “nebula” surrounding this proto-Jupiter. As other pieces of Solar system debris crossed into the Hill sphere of this nebula, they would be slowed down by friction and be captured as a satellite. Related to this is the concept of a pull down mechanism (Heppenheimer & Porco 1977). As a gas giant increases in mass from accretion (Pollack et al. 1996), the Hill sphere increases. As a subsequent effect, small Solar system bodies can possibly be captured as irregular satellites.

Dynamical capture can explain the retrograde orbits of the Jovian satellites (Nesvorný et al. 2003). The Hill sphere of a planet dictates the limit of its gravitational influence over other bodies. The theory (Nesvorný et al. 2003, 2007) states that it is impossible for a satellite to be captured in a three body system (Sun, planet and satellite). The Nice model of the Solar system (Tsiganis et al. 2005; Nesvorný et al. 2007, 2014) has a fourth body interaction placing the satellite into a stable orbit inside the Hill sphere of the gas giant. Recently the Nice model was updated to include a fifth giant planet (Nesvorný & Morbidelli 2012). This updated theory has the new planet interacting with Jupiter and allowing for the capture of the satellites, before the fifth giant planet is ejected from the Solar system. Collisions between objects could also play a part in the dynamical capture of the irregular satellites (Colombo & Franklin 1971).

The formation of the Saturnian satellite system is thought to be similarly complex. The inner satellites are possibly formed from accretion within the ring system (Charnoz et al. 2010) or from the breakup of a large, lost satellite (Canup 2010). Modeling of the Saturnian system by Salmon & Canup (2017) has shown that the mid-sized satellites could have formed from a large ice-dominated ring, with contamination of cometary material during the Late Heavy Bombardment, delivering the requisite silicate rock. Being the largest satellite in the Saturnian system, Titan is thought to have formed from accretion of proto-satellites (Asphaug & Reufer 2013). The Saturnian irregular satellites are predicted to be captured objects (Jewitt & Haghighipour 2007), though their origins are still in dispute. Collisions are thought to have played a part in

the capture of the irregular satellites of Saturn (Turrini et al. 2009). The cratering data provided by the *Cassini* spacecraft (Giese et al. 2006) supports this hypothesis.

1.4. This Project

With the discovery of several new irregular satellites (Scotti et al. 2000; Gladman et al. 2001, 2003a, 2003b; Sheppard et al. 2001, 2002, 2003a, 2003b, 2006b, 2007, 2004; Sheppard & Marsden 2003a, 2003b; Sheppard & Jewitt 2003; Sheppard & Marsden 2004; Jewitt et al. 2005; Jacobson et al. 2011; Sheppard & Williams 2012), along with the detailed examination of the Jovian and Saturnian system by the *Cassini* spacecraft (Brown et al. 2003; Porco et al. 2005, 2006; Cooper et al. 2006; Giese et al. 2006; Spahn et al. 2006; Filacchione et al. 2007, 2010, 2014, 2016, 2012; Nicholson et al. 2008; Matson et al. 2009; Buratti et al. 2010; Thomas 2010; Tosi et al. 2010; Clark et al. 2012; Spitale & Tiscareno 2012; Hirtzig et al. 2013; Brown 2014), there is an opportunity to revisit the classification of the satellite systems of the gas giants. We apply a technique called *cladistics* to characteristics of the Jovian and Saturnian satellites, in order to examine the relationships between objects in the systems. The purpose of this is twofold. First, due to their well-established classification systems, the Jovian and Saturnian satellite systems offer an opportunity to test the cladistical technique in a planetary science context. This project is an extension of Holt et al. (2016), and together they form the first use of cladistics for planetary bodies. The second aim of the project is to classify recently discovered satellites, as well as providing context for future work.

In Section 2, we introduce the cladistical technique, and how it is used in this paper. The resulting taxonomic trees for the Jovian and Saturnian systems, along with their implications for the taxonomy of the satellites, are presented in Sections 3.1 and 3.2, respectively. Section 4 discusses the implications of cladistics in a planetary science context, along with some remarks on origins of the gas giant satellites and possible future work.

2. Methods

In this section, we present an overview of the cladistical method and how it is applied to the Jovian and Saturnian satellite systems. Following a general overview of cladistics, the section progresses into the specifics of this study, including characteristics used in the paper. The section concludes with an explanation on the specific matrices of the Jovian and Saturnian satellites and how they are applied to the cladistical method.

2.1. Cladistics

Cladistics is an analytical technique, originally developed to examine the relationships between living organisms (Hennig 1965). A *clade* is the term used for a cluster of objects, or *taxa*, that are related to each other at some level. In astronomy/astrophysics, the technique has been used to look at the relationships among stars (Fraix-Burnet & Davoust 2015; Jofré et al. 2017), gamma-ray bursts (Cardone & Fraix-Burnet 2013), globular clusters (Fraix-Burnet et al. 2009), and galaxies (Fraix-Burnet et al. 2006, 2010, 2012, 2015). These works, along with this study, form a body of work in the new field of “Astrocladistics” (Fraix-Burnet et al. 2015). There are good reasons to believe that cladistics can provide sensible groupings in a planetary science context. Objects that have similar formation mechanisms should have comparable characteristics.

Daughter objects that are formed by breaking pieces off a larger object should also have similar characteristics. The advantage of this method over other multivariate analysis systems is the inclusion of a larger number of characteristics, enabling us to infer more detailed relationships.

The vast majority of work in cladistics and phylogenetics has been undertaken in the biological and paleontological sciences. Biologists and paleontologists use cladistics as a method to investigate the common origins, or “tree of life” (Darwin 1859; Hennig 1965; Hug et al. 2016), and how different species are related to one another (e.g., Van Dung et al. 1993; Salisbury et al. 2006; Říčan et al. 2011; Aria & Caron 2017; Smith et al. 2017). Historically, the investigation into relationships between different organisms reaches back to Darwin (1859). Early attempts at using tree analysis techniques occurred in the early 20th century (Mitchell 1901; Tillyard 1926; Zimmermann & Schultz 1931). Hennig (1965) is regarded as one of the first to propose “phylogenetic systematics,” the technique that would become modern cladistical/phylogenetic analysis. The technique was quickly adopted by the biological community and used to analyze every form of life, from bacteria (e.g., Olsen et al. 1994) to Dinosauria (e.g., Bakker & Galton 1974) and our own ancestors (e.g., Chamberlain & Wood 1987). Recently the use of DNA led to the expansion of the technique to become molecular phylogenetics (Suárez-Díaz & Anaya-Muñoz 2008). As computing power improves, larger data sets can be examined, and our understanding of the tree of life improves (Hug et al. 2016). For a detailed examination of the history of cladistics and pyholgenetics, we refer the interested reader to Hamilton (2014).

The cladistical methodology begins with the creation of a taxon-character matrix. Each matrix is a 2D array, with the taxa, the objects of interest, in the rows, and each characteristic in the columns. The taxa used in this study are the rings and satellites of the Jovian and Saturnian Systems. The orbital, physical and compositional properties of the rings and satellites are used as characteristics (see Section 2.2). For a given taxa, each corresponding characteristic is defined as a numerical state, usually a 0 or 1, though multiple, discrete states may be used. A 0 numerical state is used to indicate the original or “base” state. An *outgroup*, or a taxa outside the area of interest, is used to dictate the 0 base state of a characteristic. For this study, we use the Sun as an outgroup. An unknown character state can be accounted for with a question mark (?). This taxon-character matrix is created using the Mesquite software package (Maddison & Maddison 2017).

A set of phylogenetic trees are subsequently created from the Mesquite taxon-character matrix, with Tree analysis using New Technology (TNT) 1.5 (Goloboff et al. 2008; Goloboff & Catalano 2016), via the Zephyr Mesquite package (Maddison & Maddison 2015). The trees are created on the concept of maximum parsimony (Maddison et al. 1984)—that the tree with the shortest lengths, the smallest number of changes, is most likely to show the true relationships. TNT uses a method of indirect tree length estimation (Goloboff 1994, 1996) in its heuristic search for trees with the smallest length. TNT starts the drift algorithm (Goloboff 1996) search by generating 100 Wagner trees (Farris 1970), with 10 drifting trees per replicate. These starting trees are then checked, using a tree bisection and reconnection algorithm (Goloboff 1996), to generate a block of equally parsimonious trees. Closely related taxa are grouped

together in the tree. Ideally, all equally parsimonious trees would be stored, but this is computationally prohibitive. For this analysis, 10,000 equally parsimonious trees are requested from TNT, to create the tree block. Once a tree block has been generated and imported into Mesquite (Maddison & Maddison 2017) for analysis, a 0.5 majority-rules consensus tree can be constructed using a well-established algorithm (Margush & McMorris 1981). This tree is generated as a consensus of the block, with a tree branch being preserved if it is present in the majority of the trees. The resulting branching taxonomic tree is then a hypothesis for the relations between taxa, the satellites, and rings of the gas giants.

We can assess how accurately a tree represents true relationships between taxa. The number of steps it takes to create a tree is call the *tree length*. A smaller tree length implies a more likely tree, as it is more parsimonious. Tree length estimation algorithms (Farris 1970) continue to be improved, and are fully explored in a modern context by Goloboff (2015). Two other tree metrics, the consistency and retention indices, are a measure of *homoplasy*, or the independent loss or gain of a characteristic (Givnish & Sytsma 1997). High amounts of homoplasy in a tree are suggestive of random events, rather than the desired relationships between taxa (Brandley et al. 2009). Mathematically, homoplasy can be represented by the consistency index (CI) of a tree (Equation (1), Kluge & Farris 1969) and is related to the minimum number of changes (M) and the number of changes on the tree actually observed (S):

$$CI = M/S. \quad (1)$$

A tree with no *homoplasy* would have a consistency index of 1. One of the criticisms of the consistency index is that it shows a negative correlation with the number of taxa and characteristics (Archie 1989; Naylor & Kraus 1995). In order to combat the issues with the consistency index, a new measure of homoplasy, the retention index, was created (Farris 1989). The retention index (*RI*; Farris 1989) introduces the maximum number of changes (G) required into Equation (2):

$$RI = \frac{G - M}{G - S}. \quad (2)$$

As with the consistency index, a tree with a retention index of 1 indicates a perfectly reliable tree. Both of these metrics show how confidently the tree represents the most plausible relationships between taxa. Values closer to 1 of both the consistency and retention indices indicate that the tree represents the true relationships between taxa (Sanderson & Donoghue 1989). For a detailed examination of the mathematics behind the algorithms and statistics used in cladistical analysis, we direct the interested reader to Gascuel (2005).

A traditional form of multivariate hierarchical clustering is used in the detection of asteroid collisional families (Zappala et al. 1990, 1994). This method of clustering uses Gauss equations to find clusters in a parameter space, typically using semimajor axis, eccentricity, and inclination (Zappala et al. 1990). Work has also been undertaken incorporating the known colors (Parker et al. 2008) and albedo (Carruba et al. 2013) of the asteroids (Milani et al. 2014) into the classical method, though this reduces the data set significantly. The classical method of multivariate hierarchical clustering was used by (Nesvorný et al. 2003) to identify the Jovian irregular satellite families. Turrini et al. (2008) expanded the classical method into the Saturnian

irregular satellites, and utilized the Gauss equations, solved for velocities, in a similar way to Nesvorný et al. (2003) to verify the families found, using semimajor axis (a), eccentricity (e), and inclination (i) of the satellites. The rationale behind these calculations is that the dispersal velocities of the clusters would be similar to the escape velocities of the parent body. In this work we use the inverse Gauss equations, Equations (3)–(5), substituted into Equation (6), to test the dispersal velocities of the clusters found through cladistics. δa , δe , and δi are the respective differences between the individual satellites and the reference object. a_r , e_r , i_r , and orbital frequency (n_r) are parameters of the reference object. In this case, the reference object is taken as the largest member of the cluster. The true anomaly (f) and perihelion argument ($w + f$) at the time of disruption are unknown. Only in special cases (e.g., for young asteroid families; Nesvorný et al. 2002) can the values of (f) and ($w + f$) be inferred from observations. In this work we adopt $f = 90^\circ$ and $(f + w) = 45^\circ$, respectively, as reasonable assumptions. Previous works by Nesvorný et al. (2003) and Turrini et al. (2008) using this method do not specify the true anomaly (f) and perihelion argument ($w + f$) used, nor the central reference point, making any comparisons between them and this work relative rather than absolute. The final δV_d for the cluster is composed of the velocities in the direction of orbital motion (δV_T), the radial direction (δV_R), and perpendicular to the orbital plane (δV_W):

$$\delta V_T = \frac{n_r a_r (1 + e_r \cos f)}{\sqrt{1 - e_r^2}} \cdot \left[\frac{\delta a}{2a_r} - \frac{e_r \delta e}{1 - e_r^2} \right] \quad (3)$$

$$\delta V_R = \frac{n_r a_r}{(\sqrt{1 - e_r^2}) \sin f} \cdot \left[\frac{\delta e_r (1 + e_r \cos f)^2}{1 - e_r^2} - \frac{\delta a (e_r + e_r \cos^2 f + 2 \cos f)}{2a_r} \right] \quad (4)$$

$$\delta V_W = \frac{\delta i \cdot n_r a_r}{\sqrt{1 - e_r^2}} \cdot \frac{1 + e_r \cos f}{\cos(w + f)} \quad (5)$$

$$\delta V_d = \sqrt{\delta V_T^2 + \delta V_R^2 + \delta V_W^2}. \quad (6)$$

Cladistics offers a fundamental advantage over this primarily dynamics based clustering, via the incorporation of unknown values. Classical multivariate hierarchical clustering (Zappala et al. 1990) requires the use of a complete data set, and as such a choice is required. The parameters are either restricted to only known dynamical elements, or the data set is reduced to well-studied objects. Cladistical analysis can incorporate objects with large amounts of unknown information, originally fossil organisms (Cobbett et al. 2007), without a reduction in the number of parameters.

2.2. Characteristics

We define 38 characteristics that can be broken into three broad categories: orbital, physical, and compositional parameters. All numerical states are considered to have equal weight. The discrete character sets are unordered. Any continuous characteristics are broken into bins, as cladistical analysis requires discrete characteristics. We developed a Python program to establish the binning of continuous characteristics. The pandas Cut module (McKinney 2010) is used to create the bins. Characteristics are binned independent of each other and for each of the Jovian and Saturnian systems.

The aforementioned Python program iterates the number of bins until a linear regression model between binned and unbinned sets achieves a coefficient of determination (r^2) score of >0.99 . This is calculated using the stats package in SciPy (Jones et al. 2001). Thus each character set will have a different number of bins, r^2 score, and delimiters. All characteristics are binned in a linear fashion, with the majority increasing in progression. The exception to the linear increase is the density character set, with a reversed profile. All of the continuous, binned characteristic sets are ordered, as used by Fraix-Burnet et al. (2006). A full list of the characteristics used, the r^2 score for each of the binned characteristics, along with the delimiters are listed in Appendix A.

The first broad category includes the five orbital characteristics (Appendix A.1). This category is composed of two discrete characteristics: presence in orbit around the gas giant and prograde or retrograde orbit. The three remaining characteristics—semimajor axis (a), orbital inclination (i), and eccentricity (e)—are continuous and require binning using the aforementioned Python program.

The second category used to construct the matrix consists of two continuous physical characteristics, density, and visual geometric albedo (Appendix A.2). We chose to not include mass, or any properties related to mass, as characters in the analysis. The inclusion of these characteristics could hide any relationships between a massive object and any daughter objects, as the result of collisions.

The third category describes the discrete compositional characteristics and details the presence or absence of 31 different chemical species (Appendix A.3). In order to account for any positional bias, the fundamental state, solid, liquid, gas, or plasma was not considered. In this analysis, we make no distinction between surface, bulk, and trace compositions. This is to account for the potential of daughter objects to have their bulk composition comprising surface material from the parent. The majority of compounds have absence as a base state (0) and presence as the derived (1). The exceptions are the first three molecules—elemental hydrogen (eH), hydrogen (H_2), and helium (He)—all of which are found in the Sun. As the Sun is the designated outgroup, the base state (0) indicates the presence of these species. With the exception of elemental hydrogen, the remaining single element species are those found in compounds. The spectroscopy of an object often only reports on the presence of an ion, as opposed to a full chemical analysis. As more detailed analysis becomes available, characters may be added to the matrix. Several chemical species are used in this particular matrix that are either not present in any of the satellites or unknown. These are included for future comparisons with other orbital bodies.

2.3. Matrices

The Jovian taxon-character matrix holds 68 taxa consisting of the Sun (outgroup), 4 inner satellites, the main ring, 4 Galilean satellites, and 59 irregular satellites. Appendix B (Table 3) contains the matrix, along with the references used in its construction.

The Saturnian matrix, presented in Appendix C (Table 4), is created with 76 taxa. These taxa are the Sun (outgroup), 6 main rings, 9 inner small satellites, 4 minor rings, 8 large icy satellites, 4 Trojan satellites, 3 Alkynoids and their associated rings, and the 38 irregular satellites. The references used in the construction of the Saturnian matrix are located in Appendix C. Both

matricies use the same characteristics, as discussed in Section 2.2, and are available in machine readable format.

3. Results

In this section we present the resulting taxonomic trees from the analysis of the Jovian and Saturnian satellites. The taxonomic trees are used to form the systematic classification of the Jovian (Table 1) and Saturnian (Table 2) satellite systems. Using inverse Gauss equations (Zappala et al. 1990), in a similar method to Nesvorný et al. (2003) and Turrini et al. (2008), we show in Tables 1 and 2 dispersal velocities (δV) for each of the taxonomic groups where a single origin object is hypothesized—namely the irregular satellites. For these calculations we assume the largest representative of the cluster as the origin point. See Section 2.1 for further discussion.

3.1. Jovian Taxonomy

The results of the cladistical analysis of the individual Jovian satellites are shown in Figure 1. This 0.5 majority-rules consensus tree has a tree length score of 128, with a consistency index of 0.46 and a retention index of 0.85. The low value of the consistency index is possibly due to the mixed use of ordered, multi-state, continuous characteristics and bi-modal compositional characteristics (Farris 1990). The high retention index suggests that the consensus tree is robust and demonstrates the most likely relationships between the satellites.

As can be seen in the Jovian taxonomic tree in Figure 1, the satellites cluster into clades resembling the taxonomy proposed by Nesvorný et al. (2003) and Sheppard & Jewitt (2003). The irregular satellites are a separate cluster to the prograde regular satellites.

We maintain the closest family to Jupiter, the Amalthea family, as a valid taxonomic cluster. The dispersal velocity is very large and may suggest that the Amalthea family did not form from a single object. This family, along with Jupiter’s main ring, is associated with the well-known Galilean family.

In the analysis, we maintain the “irregular” satellite group. The Himalia family clusters with the retrograde satellites, separate to the other prograde satellites. The Himalia family has relatively low inclinations in comparison with the Jovian retrograde satellites, and their high eccentricity could be explained by disruptions (Christou 2005). The small satellites Themisto and Carpo cluster together with the other prograde satellites in the Himalia family. We propose that Themisto and Carpo be included in the Himalia family, as they are the sole members of the groups proposed by Sheppard & Jewitt (2003), and show similar orbital characteristics. The large mean dispersal velocity calculated for the Himalia family (see Table 1) was also noticed by Nesvorný et al. (2003) for the Prograde satellites. The large mean dispersal velocity is due to the dispersal velocities of Themisto and Carpo. Without including these members, the mean dispersal velocity for the classical Himalia family is $154.6 \pm 72.5 \text{ m s}^{-1}$, close to the escape velocity of Himalia (121.14 m s^{-1}). This dispersal velocity of the classical Himalia family was explained via gravitational scattering from Himalia by Christou (2005). Disruption and scattering could also be used to explain the large dispersal velocities of Themisto and Carpo, though further modeling is required.

The term “irregular” is maintained through the retrograde family for consistency with the literature (Nesvorný et al. 2003, 2004; Sheppard & Jewitt 2003; Beaugé & Nesvorný 2007;

Jewitt & Haghighipour 2007). The retrograde irregular satellites are a separate but related cluster to the Himalia, prograde irregulars. The broad classifications introduced by Sheppard & Jewitt (2003) and Nesvorný et al. (2003) are preserved, though the Ananke/Carme family is unresolved and may be split into subfamilies. Separating out the traditional families (Nesvorný et al. 2003; Sheppard & Jewitt 2003; see colors in Figure 1) gives smaller dispersal velocities. The traditional Ananke (escape velocity (eV) 23.10 m s^{-1}) family has a δV of $61.0 \pm 45.6 \text{ m s}^{-1}$, traditional Carme (eV 29.83 m s^{-1}) has $36.2 \pm 13.1 \text{ m s}^{-1}$, and a created Sinope (eV 27.62 m s^{-1}) family has $323.9 \pm 97.3 \text{ m s}^{-1}$. These are smaller than the δV of our unresolved Ananke/Carme Family ($457.2 \pm 445.7 \text{ m s}^{-1}$; see Table 1). Nesvorný et al. (2003) used similar small δV values to establish the Ananke and Carme dynamical families. The dynamical situation could be explained through a more recent capture and breakup event for Ananke, Carme, and Sinope that disrupted the ancestral irregular satellites. The identified Iocaste and Pasiphae families also have large dispersal velocities, suggestive of disruptions. Following the nomenclature of Sheppard & Jewitt (2003), each of the families and subfamilies are represented by the name of the largest contained satellite. Satellites within families are related by their retrograde orbit, high inclinations, and eccentricities. In addition to their linked orbital characteristics, the satellites of the retrograde irregular group all show a low albedo (Beaugé & Nesvorný 2007).

The Ananke subfamily is tightly constrained in its orbital characteristics, with a small dispersal velocity. While the characteristics listed in Table 1 would preclude them from being included in the Pasiphae family, their clustering around a common semimajor axis, inclination, and eccentricity suggest that they are a distinct young dynamical family. The members we include in the Ananke family for this analysis are all historical members of the family (Jewitt & Haghighipour 2007). Some of the satellites that have been historically included in the Ananke family (Jewitt & Haghighipour 2007) are moved to other families. We do not add any new satellites to this family.

The orbital characteristics of the Carme subfamily are tightly constrained. Satellites in this family orbit further from Jupiter, with higher orbital inclinations, but similar eccentricities to the Ananke family. As with the Ananke family, it is the highly constrained orbital characteristics and low mean dispersal velocity that justify the classification of this traditional family (Jewitt & Haghighipour 2007). According to the tree presented in Figure 1, there is a continuum between the Ananke and Carme families. However, differences in orbital characteristics, broken down in Table 1, distinguish both of these families from each other.

A new cluster, the Iocaste family, is defined as shown in Figure 1 and Table 1. The semimajor axis of this family spans most of the orbital space where irregular satellites have been discovered. The lower eccentricities and albedo are used to separate this family from the Pasiphae family. As with the Pasiphae family, the Iocaste family has a high mean dispersal velocity (510.2 ± 303.3 compared with a escape velocity of 3.16 m s^{-1}), suggestive of disruptions taking place at some point since the breakup of the original object (Christou 2005). Iocaste, being the largest member of this family, is proposed as the representative object. Also included are several members that have been previously included in other families (Jewitt & Haghighipour 2007), along with new unnamed satellites. For full details on included satellites and the descriptive properties of the family, see Table 1.

Table 1
Jovian Satellite Systematic Classification

Taxonomy	Members	Orbit	Semimajor Axis (km)	Inclination	Eccentricity	Density (kg m^{-3})	Albedo	Composition	Velocity (δV) (m s^{-1})	References
Amalthea family	Thebe, Amalthea, Metis, andAdrastea	Prograde	$<3.0 \times 10^5$	$<0^\circ 02$	$<2^\circ$	<900	<0.1	Predominately water ice and silicates	3570.4 ± 491.8	1
Galilean family	Io, Ganymede, Europa, and Callisto	Prograde	4.0×10^5 – 2.0×10^6	$<0^\circ 5$	<0.01	>1800	>0.18	Water ice and silicates dominate; presence of SO_2 ; other chemical species present.	...	2
Jovian irregular satellite group										
Himalia family	Leda, Elara, Lythea, Himalia, and Themisto	Prograde	7.5×10^6 – 1.8×10^6	25° – 55°	0.1–0.3	...	<0.1	Silicate-based	623.8 ± 750.3	3, 4
Ananke/Carme family	S/2003 J3, S/2003 J9, Ananke subfamily, Carme subfamily, and Sinope subfamily	Retrograde	1.88×10^7 – 2.5×10^7	143° – 166°	0.2–0.4	...	<0.07	...	457.2 ± 445.7	3, 4
Ananke subfamily	Euanthe, Thyone, Mneme, Harpalyke, Praxidike, Thelxinoe, and Ananke	Retrograde	2.0×10^7 – 2.15×10^7	145° – 152°	0.2–0.25	...	<0.07	...	61.0 ± 45.6	3, 4
Carme subfamily	Arche, Pasithee, Chaldene, Isonoe, Kale, Aitne, Erinome, Taygete, Carme, Kalyke, Eukelade, and Kallichore	Retrograde	2.2×10^7 – 2.4×10^7	164° – 166°	0.24–0.27	...	<0.07	...	36.1 ± 13.1	3, 4
Sinope subfamily	Eurydome, Autonoe, Sinope, and Callirrhoe	Retrograde	2.2×10^7 – 2.42×10^7	147° – 159°	0.27–0.35	...	<0.06	...	323.9 ± 97.3	
Iocaste family	Euporie, S/2003 J18, Hermippe, Helike, Iocaste, S/2003 J15, Herse, S/2003 J4, Aoede, S/2003 J5, and S/2003 J10	Retrograde	1.9×10^7 – 2.5×10^7	140° – 165°	0.1–0.45	...	<0.05	...	510.2 ± 303.3	
Pasiphae family	S/2003 J12, S/2011 J1, S/2010 J2, S/2003 J19, S/2010 J1, S/2011 J2, Sponde, Pasiphae, Megaclite, Hegemone, S/2003 J23, Cyllene, Kore, and S/2003 J2	Retrograde	1.9×10^7 – 2.9×10^7	145° – 164°	0.30–0.421	...	<0.1	...	412.3 ± 224.5	3, 4

References. (1) Barnard (1892), (2) Galilei (1610), (3) Nesvorný et al. (2003), (4) Sheppard & Jewitt (2003).

Table 2
Saturnian Satellite Systematic Classification

Taxonomy	Members	Orbit	Semimajor Axis (km)	Inclination	Eccentricity	Density (kg m ⁻³)	Albedo	Composition	Velocity (δV) (m s ⁻¹)	References
Saturnian inner system group, main ring and icy satellites	Atlas, Janus, Epimetheus, Prometheus, Janus/Epimetheus ring, G-ring, D-ring, Pan, Aegaeon, S/2009 S1, F-ring, B-ring, Cassini division, C-ring, Daphnis and A-ring. Possible members: Telesto, Calypso, Methone ring arc, Anthe ring arc, Pallene ring arc, Methone, Anthe, Pallene, Polydeuces Mimas, Tethys, Enceladus family, Hyperion, Titan, and Iapetus; see Section 3.2 for discussion.	Prograde	$<4.0 \times 10^6$	$<15^\circ$	<0.03	550–1900	0.1–1	Composition of water ice with silicates and presence of CO ₂ . Other chemical species may be present.	...	1, 2
Enceladus family	E-ring, Enceladus, Rhea, Dione, and Helene	Prograde	1.8×10^5 – 5.3×10^5	$<0.5^\circ$	0	1200–1700	>0.7	Complex composition, predominately water ice and silicates, with hydrocarbons and CO ₂ present	...	
∞ Saturnian irregular satellite group										
Albiorix family	Bebhionn, Erriapus, Albiorix, and Tarvos	Prograde	1.6×10^7 – 1.8×10^7	30° – 40°	0.4–0.6	...	<0.1	...	80.9 ± 1.6	3, 4, 5
Siarnaq family	Tarqeq, Kiviuq, Ijiraq, Paaliaq, and Siarnaq	Prograde	1.1×10^7 – 1.9×10^7	40° – 50°	0.1–0.4	...	<0.1	...	266.8 ± 60.0	3, 4, 5
Phoebe family	Phoebe ring, Phoebe, Fenrir, Loge, Aegir subfamily, and Ymir subfamily	Retrograde	1.1×10^7 – 2.51×10^7	$>145^\circ$	>0.1	...	<0.1	...	763.3 ± 259.0	3, 4, 5
Aegir subfamily	S/2007 S2, Mundilfari, Jarnsaxa, S/2006 S1, Bergelmir, Suttungr, Farbauti, S/2007 S3, Aegir, and Fornjot	Retrograde	1.6×10^7 – 2.51×10^7	$>150^\circ$	0.1–0.25	295.1 ± 125.0	5
Ymir subfamily	Skathi, Skoll, Greip, Hyrrokkin, S/2004 S13, S/2004 S17, Narvi, S/2004 S12, S/2004 S07, Hati, Bestla, Thrymr, S/2006 S3, Kari, Surtur, and Ymir	Retrograde	1.55×10^7 – 2.30×10^7	$>145^\circ$	0.25–0.6	...	<0.1	...	497.5 ± 247.7	5

References. (1) Huygens (1659), (2) Cassini (1673, 1686), (3) Nesvorný et al. (2003), (4) Sheppard & Jewitt (2003), (5) Turrini et al. (2008).

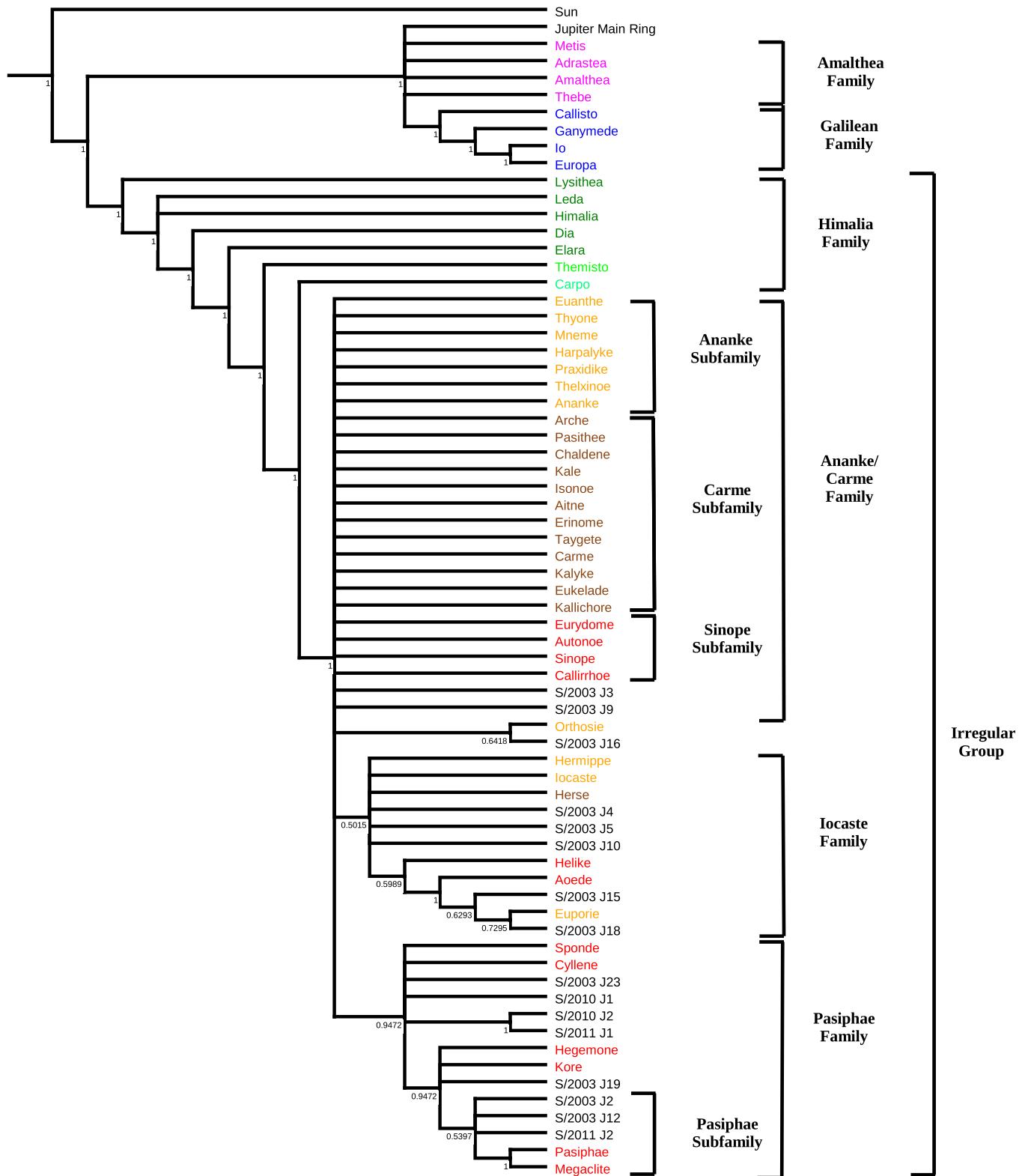


Figure 1. Majority consensus taxonomic tree of objects in the Jovian system. This tree has a tree length score of 128, with a consistency index of 0.46 and a retention index of 0.85. Numbers indicate the frequency of the node in the 10,000 most parsimonious tree block. Colors represent the terminology used in traditional classification: Amalthea inner regular family, Galilean family, Themisto prograde irregular, Himalia prograde irregular, Carpo prograde irregular, Ananke irregular family, Carme irregular family, Pasiphae irregular group, and unnamed and unclassified. Proposed groups and families are shown on the right.

The Pasiphae family shows a broad range of orbital characteristics that, along with the large dispersal velocity (412.3 ± 224.5 compared with an escape velocity of 47.16 m s^{-1}), are suggestive of disruptions during the family's

lifetime (Christou 2005). The Pasiphae family has a broad range of semimajor axes and inclinations, with the Pasiphae family orbiting further from Jupiter and having larger eccentricities on average than the new Iocaste family (see

Table 1). A Pasiphae subfamily (see Figure 1), with a δV of $230.1 \pm 174.3 \text{ m s}^{-1}$, can be identified. This may imply a secondary, more recent breakup from Pasiphae. In addition, many of the unnamed satellites from recent observations (Gladman et al. 2003a, 2003b; Sheppard et al. 2003b, 2003a, 2004; Sheppard & Marsden 2003a, 2003b, 2004; Jacobson et al. 2011; Sheppard & Williams 2012) are associated with this family; see Table 1 and Figure 1 for a complete list.

3.2. Saturnian Taxonomy

Cladistical analysis of the Saturnian system yields the 0.5 majority-rules consensus tree (Figure 2), constructed from the 10,000 parsimonious trees, with a tree length score of 186. The tree has a consistency index of 0.30 and a retention index of 0.81. The consistency index of the Saturnian tree is lower than that of the Jovian tree, though this could be due to the number of taxa used (Sanderson & Donoghue 1989). As with the Jovian tree, this low consistency index could be due to the mixed character states. This effect is to be explored further in a future paper. The high retention index indicates that the tree is suggestive of the true relationships (Farris 1989).

The tree shown in Figure 2 highlights the diversity of structures found in the orbit of Saturn. Satellites cluster into two main groupings around Saturn: the Inner group, comprised of rings and icy satellites, and the Irregular satellite group (see Table 2 for members and diagnostic properties of each clade). While the traditional classification nomenclature (Nesvorný et al. 2003; Sheppard & Jewitt 2003; Jewitt & Haghighipour 2007) is broadly conserved, several discrepancies require discussion. Table 2 shows our new taxonomy, along with included members of the families and their descriptive properties.

The Main ring and Icy satellite group form an unresolved, inner system group. This group includes the Saturnian ring system, the Alkynoids and their associated ring arcs, as well as the larger Icy satellites and their Trojans. We have confirmed the recently discovered S/2009 S1 (Spitale & Tiscareno 2012) is part of this group due to its orbital characteristics. Within this large group, there is the resolved Enceladus family.

Our results suggest the traditionally classified Alkyonides, Methone, Anthe, and Pallene, along with their associated rings, are not clustered with the the Enceladus family, as would be expected by their orbital location, between Mimas and Enceladus, within the E-ring. Due to their bulk water ice composition, the Alkyonides associate with the Main ring objects (see Figure 2). The low density and mid-range albedo of Pallene and Methone (Hedman et al. 2009) suggest that the association with the Main ring group is genuine. The dynamic resonances of both Methone and Anthe (Callegari & Yokoyama 2010) imply that these objects were captured, rather than forming in situ. As there is very little known about the composition of these objects, beyond their bulk water ice composition (Hedman et al. 2009), further study and dynamical modeling of the capture process is required to resolve their true origins.

Like the Alkynoids, the Trojan satellites of Tethys, Calypso, and Telesto also form an association with the main rings. The reason for this could be that Calypso and Telesto, like the Alkynoids, are also possible captured main ring objects. The capture dynamics could be similar to that of the Jovian Trojan asteroids (Morbidelli et al. 2005; Lykawka & Horner 2010; Nesvorný et al. 2013). Both the Tethys Trojans (Buratti et al. 2010) and main ring objects are chiefly composed of water ice,

implying a common origin. The bulk composition of Tethys is also prominently water ice (Buratti et al. 2010), with a very small fraction of silicates. Trojans may instead have formed from the same material as Tethys itself, either during accretion (Charnoz et al. 2011) or in the same orbit from a large debris disk (Canup 2010). As Tethys is also in the unresolved Main ring and Satellite group, we cannot differentiate between the two scenarios. Further compositional information about the Tethys Trojans could shed light on this issue. Polydeuces, a Trojan of Dione, also forms an association with the Main ring group in our analysis. This could be due to overemphasis on orbital and physical characteristics, since the bulk composition of Polydeuces is unknown (Thomas et al. 2013). Helene, the more well-studied Trojan of Dione (Thomas et al. 2013), is well within the Enceladus Family. Helene and Dione are closely associated in our analysis, implying that Helene is a daughter object of Dione.

The outer icy satellites, Titan, Hyperion, and Iapetus, do not form a single cluster, and are therefore not considered a valid taxonomic group. They are associated with the Main ring and Icy satellite group. The Enceladus family is formed by the known association of the E-ring, Enceladus, and Icy satellites (Verbiscer et al. 2007), which is mainly due to the detection of volatile chemicals, such as NH_3 , CH_4 , and other hydrocarbons. Plumes from Enceladus containing these chemicals (Porco et al. 2006), thought to be representative of the subcrust ocean (Porco et al. 2006), are the source of the E-ring (Spahn et al. 2006). Titan itself also has an abundance of these volatiles (Hirtzig et al. 2013), implying a possible association between the Icy satellites of Saturn that remains unresolved in our analysis. Material from the outer satellites, particularly Pheobe and its associated ring (Tosi et al. 2010; Tamayo et al. 2011), is thought to play a role in the observed hemispherical dichotomy on Iapetus (Tosi et al. 2010). In Figure 2, Iapetus is unresolved in the Main ring and Icy satellite group.

The irregular satellites form a major cluster with each other separate from the inner Saturnian system, and are therefore collected under the Irregular satellite group. Along with their high inclinations, eccentricities, and semimajor axes, the Irregular satellite group is characterized by a dark albedo, comparative to the other objects in the Saturnian system. We follow the naming convention introduced with the Jovian satellites (Section 3.1), where each irregular satellite family is represented by the largest member (Jewitt & Haghighipour 2007). We therefore rename the classical Inuit group (Blunck 2010) as the Siarnaq family and the Gallic group (Blunck 2010) as the Albiorix family. Though this does change the formal name of the clusters, we encourage the discoverers of the unnamed satellites (Gladman et al. 2001; Sheppard et al. 2003a, 2006b, 2007; Jewitt et al. 2005) and any future discoveries that are placed in these groups, to follow IAU convention and use names from Inuit and Gallic mythology for satellites in the Siarnaq and Albiorix families, respectively. As in Turrini et al. (2008), the Albiorix family is distinct and has a low mean dispersal velocity (δV). The Siarnaq family has a higher δV , again suggestive of disruptions (Christou 2005). The mean δV of all prograde satellites is $364.8 \pm 114.9 \text{ m s}^{-1}$, only slightly higher than that of the Siarnaq family (Turrini et al. 2008). This could imply a disruption scenario, with a more recent capture of the Albiorix family parent body disrupting the older Siarnaq family. Our cladistical analysis supports this scenario, as the Siarnaq family shows a more branching structure than the Albiorix family. Further compositional information about these bodies, as well as dynamical modeling, could resolve this complex situation. In our

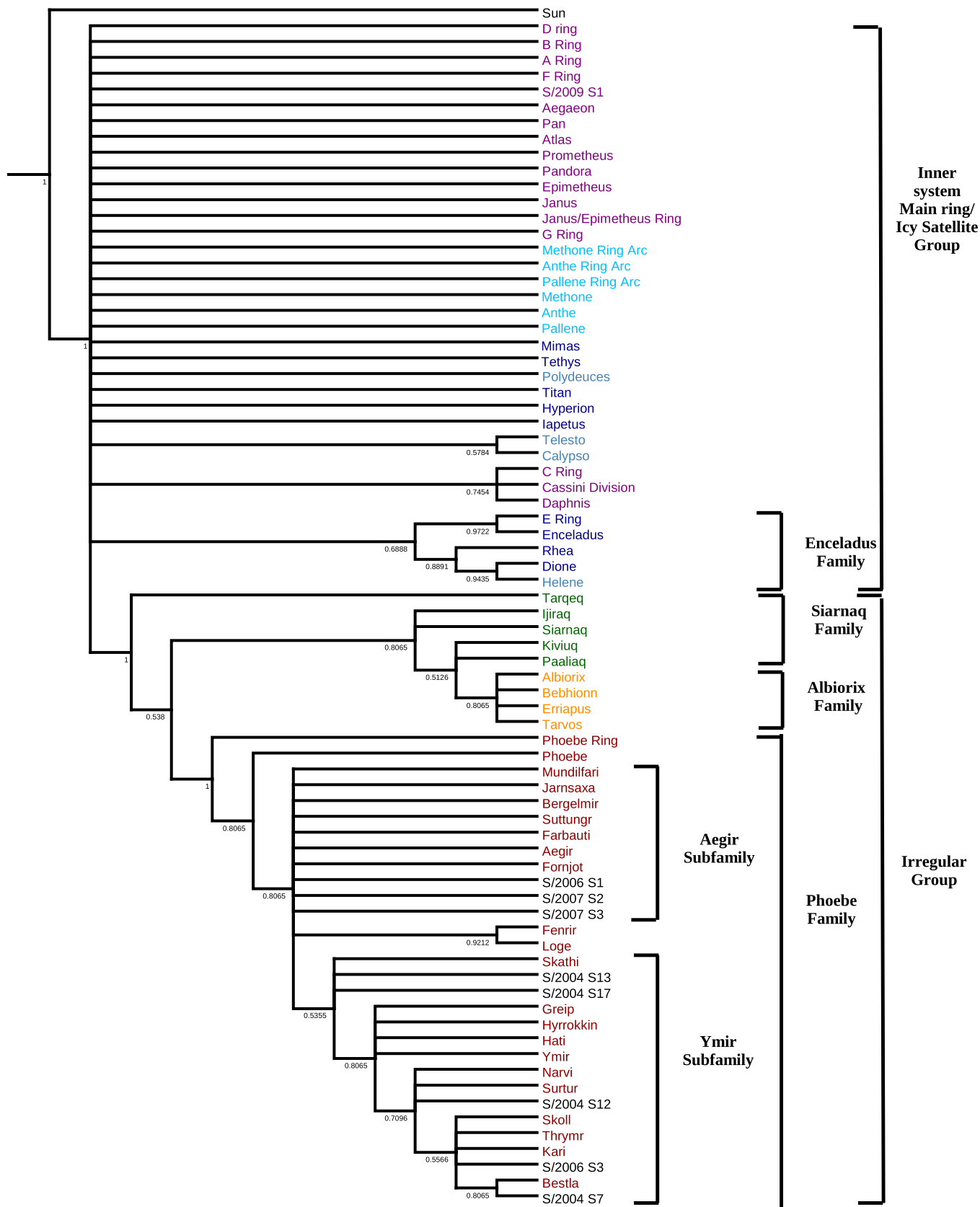


Figure 2. Majority Consensus taxonomic tree of objects in the Saturnian system. The tree has a consistency index of 0.30 and a retention index of 0.81. Numbers indicate frequency of the node in the 10,000 most parsimonious tree block. Colors represent terminology used in classical classification: the main ring group, with associated shepherd satellites; mid-sized icy satellites and Titan; Trojan satellites; alkanoids and associated rings; “Inuit” prograde irregular family; “Gallic” prograde irregular family; “Norse” retrograde irregular family; and unnamed and unclassified. Proposed groups and families are shown to the right.

analysis, we separate out the retrograde irregular satellites, including Phoebe, from the prograde irregular satellites. In previous taxonomy, this group has been classified as the “Norse” group (Blunck 2010). In our revised nomenclature, this group should be termed the Phoebe family. We further separate out two clades, distinct from Phoebe and its associated ring. The first clade, the unresolved Aegir subfamily (previously identified as the S/2004 S10 group in Turrini et al. 2008), is characterized as having, on average, orbits further from Saturn, with low eccentricities and higher inclinations. The second clade is the Ymir subfamily and is categorized, on average, by being closer to Saturn, but with high eccentricities. This subfamily shows a branching structure and may be further split (Grav & Bauer 2007). This family was also identified by Turrini et al. (2008). We identify an association between Fenrir and Loge, with a low dispersal velocity ($\delta V = 114.4 \text{ m s}^{-1}$), suggestive of a recent breakup. The high dispersal velocity (δV) of the Phoebe family is due to the selection of Phoebe as a reference point. If Phoebe and the associated ring are removed from the family, and Ymir (with an escape velocity of 8.56 m s^{-1}) is selected as the reference object, the δV is halved from $763.3 \pm 259.0 \text{ m s}^{-1}$ to $439.9 \pm 215.1 \text{ m s}^{-1}$. The satellite with the lowest δV to Phoebe is S/2007 S2, with $\delta V = 248.0 \text{ m s}^{-1}$, still significantly larger than the escape velocity of Phoebe (100.8 m s^{-1}). Turrini et al. (2008) also found a dynamical separation between Phoebe and the other retrograde satellites. This is supportive of the narrative that Phoebe has a different origin than the other retrograde irregular satellites of Saturn (Turrini et al. 2008). The high δV among all the subfamilies shows that a complex dynamical situation is present in the Saturnian irregular satellites. Phoebe has been shown to clear its orbital parameter space (Turrini et al. 2008), which could have had a major disruptive effect on those remaining satellites (Turrini et al. 2008). The similarities between our analysis and that of Turrini et al. (2008) further validate cladistics as a method suitable for applications in Solar system astronomy. The addition of detailed compositional information from the other irregular satellites to an updated cladistical analysis could solve some of the minor discrepancies found between this analysis and that of Turrini et al. (2008).

We assign the currently unnamed irregular satellites to each of the subfamilies. S/2006 S1, S/2007 S2, and S/2007 S3 are part of the Aegir subfamily. We include S/2004 S13, S/2004 S17, S/2004 S12, S/2006 S3, and S/2007 S7 in the Ymir subfamily. See Table 2 for a full list of members in each subfamily. As with the Albiorix and Siarnaq families, we encourage discoverers of new satellites that fall within the Phoebe family to follow the Norse mythological naming convention as set by the IAU.

4. Discussion

In this study we have shown, using the Jovian and Saturnian satellite systems, that cladistics can be used in a planetary science context. We have ensured that the technique is objective by statistically creating bins for characteristics that are continuous in nature (see Section 2.2). By thus ensuring the objectivity of our analysis, we increase the confidence that cladistics is a valid technique that can be applied in the planetary sciences. Our results largely support the traditional classifications used in both the Jovian and Saturnian systems. However, the power of cladistics is shown in the ease of classifying new satellites, as well as identifying substructures within larger clusters. Cladistics also offers a method of analysis where limited information is available.

In our study we have examined well-studied satellites, as well as those where only dynamical information is available. In traditional methods of analysis, either only dynamical information is considered, or the data set is truncated in favor of more well-studied bodies. Cladistics offers a method that can incorporate as much information about an object as is available, while accounting for any unknown characteristics. As more detailed information becomes available, either of known or newly discovered satellites, cladistics offers a systematic method for inclusion or revision of the classification system.

The relationships that we noted between the satellites suggest common formation scenarios within the clusters. The prograde, inner families of Jupiter are the products of accretion from a circumplanetary disk (Canup & Ward 2002). The association of the Amalthea and Galilean families, along with the Main ring of Jupiter, in our analysis supports this hypothesis. Clustering of the Himalia family with other “irregular” satellites implies a capture scenario. The prograde nature of the Himalia family is possibly explained via a nebula drag capture mechanism (Ćuk & Burns 2004). Further modeling of the Himalia family is required to ascertain their true origins, particularly in light of the Jovian pebble formation hypothesis that may not include an extended nebula (Levison et al. 2015).

With the proposal that Sinope forms its own subfamily, each Jovian irregular satellite subfamily contains only a single large satellite. This strengthens the hypothesis that each of the families represents a capture event and subsequent breakup (Nesvorný et al. 2007) of an object external to the Jovian system. Two of the subfamilies, the Pasiphae and Sinope subfamilies, show a broad range of orbital characteristics and larger dispersal velocities. The other two, the Ananke and Carme subfamilies, show much more constrained characteristics and smaller dispersal velocities. This dichotomy between the two types of subfamilies, broad versus constrained, could imply at least two capture events, with the earlier Pasiphae and Sinope families being disrupted by later Ananke and Carme captures. The Iocaste family does not contain a large progenitor satellite, but has high dispersal velocities. This is suggestive of a possible ejection scenario. An alternative hypothesis is that the capture events happen simultaneously, but there were multiple disruption events. Both scenarios are supported by the dichotomy in dispersal velocities. Future analysis and simulations into the origins of the irregular satellites could help determine which theory is more probable.

As with the Jovian satellites, there are multiple origins for the origin of the Saturnian rings and satellites. The results from our analysis support a growing body of work showing the complexity of formation scenarios in the Saturnian system. The rings themselves possibly formed after the breakup of an inner icy satellite (Canup 2010).

The unresolved nature of the inner Saturnian system shows a complexity of formation scenarios. The main ring satellites, along with the Alkyonides and Tethys Trojans, possibly formed via accretion from the current ring system (Charnoz et al. 2010). The Alkyonides and Tethys Trojans are then secondarily captured in their current orbits. The major icy satellites, those in the E-ring and outer satellites, probably formed in an accretion scenario, with delivery of the silicate from the outer system (Salmon & Canup 2017). Titan could be secondarily derived from multiple subsatellites that formed in the same disk (Asphaug & Reufer 2013). The volatiles are delivered from comets, with at least one, Phoebe, being captured in orbit. The size of Phoebe is not

traditionally associated with comet nuclei, but at least one comet, C/2002 VQ94, with a similar 100 km diameter has been observed (Korsun et al. 2014). The irregular satellite families and subfamilies form from collisional breakup events (Nesvorný et al. 2004) resulting from the captured comet nuclei. The large dispersal velocities of the subfamilies imply that this capture and disruption process is complex and requires detailed modeling.

We have shown that cladistics can be used in the classification of the Jovian and Saturnian satellite systems. Consequently, several related studies may be attempted in the future. Uranus and Neptune have similarly complex satellite systems as those of Jupiter and Saturn (Jewitt & Haghighipour 2007). These satellite systems could also be classified using cladistics, particularly the irregular satellites. Such a study is hampered by a lack of completeness in the irregular satellite data set (Sheppard et al. 2005, 2006a), but may become practical as observational technology improves and the hypothesized small irregular satellites are discovered. Cladistics could be used to further investigate the origins of the irregular satellites of Saturn and Jupiter. As the irregular satellites are thought to be captured bodies (e.g., Nesvorný et al. 2007), the question becomes from which small body population they originated. Comparisons between the well-studied irregular satellites and other Solar system bodies could help constrain the origins of these satellites.

5. Conclusions

We have shown that the new application of cladistics on the Jovian and Saturnian satellite systems is valid for investigating the relationships between orbital bodies. In the Jovian system, the traditional classification categories (Nesvorný et al. 2003; Sheppard & Jewitt 2003; Jewitt & Haghighipour 2007) are preserved. We support the hypothesis put forward by Nesvorný et al. (2007) that each Jovian irregular satellite family can be represented by the largest member, and that each family comprises the remnants of a dynamical capture event and subsequent breakup. We can also assign recently discovered, as yet unnamed, satellites to each of their respective Jovian families. Cladistical analysis of the Saturnian system broadly preserves the traditional classifications (Nesvorný et al. 2003; Sheppard & Jewitt 2003; Jewitt & Haghighipour 2007; Turrini et al. 2008), strengthening the validity of the cladistical method. In the Phoebe family of retrograde, irregular satellites, we assign two subfamilies similar to those found by Turrini et al. (2008). We rename the classical

mythological designations for the Saturnian irregular satellites, to represent the largest member of the subfamily, in order to be consistent with the Jovian naming convention. Newly discovered, unnamed Saturnian satellites are easily assigned to various subfamilies. Through the application of the technique to the Jovian and Saturnian systems, we show that cladistics can be used as a valuable tool in a planetary science context, providing a systematic method for future classification.

This research was in part supported by the University of Southern Queensland’s Strategic Research Initiative program. We wish to thank an anonymous reviewer for his/her comments, particularly on Multivariate Hierarchical Clustering. The AAS Statistics Reviewer provided valuable feedback on the methodology. Dr. Guido Grimm assisted with the cladistical methodology and terminology used in this paper. Dr. Pablo Goloboff provided assistance with TNT, which is subsidized by the Willi Hennig Society, as well as additional comments on the methodology. We would like to thank Dr. Henry Throop for discussions regarding the Ring systems.

Software: Mesquite 3.10 (Maddison & Maddison 2017), Python 3.5, Spyder 2.3.8 (Spyder Development Team 2015), Anaconda Python distribution package 2.40 (Continuum Analytics 2016), pandas Python package (McKinney 2010), ScyPy Python package (Jones et al. 2001), TexMaker 4.1.1, Tree analysis using New Technology (TNT) 1.5 (Goloboff et al. 2008; Goloboff & Catalano 2016), Zephyr 1.1: Mesquite package (Maddison & Maddison 2015).

Appendix A List of Characteristics

Below you will find a list of characters used in the creation of the Jovian (Appendix B) and Saturnian (Appendix C) satellite matrices. See Section 2.2 for a full discussion.

A.1. Orbital Characteristics

1. In orbit around the gas giant (Orb): no (0); yes (1)
2. Revolution (Rev): Prograde revolution(0); Retrograde revolution (1)
3. Semimajor axis(a):
 - (i) Jovian: r^2 :0.990 Bin delimiters 0 km (0); 3.67892625×10^6 km (1); 7.2348525×10^6 km (2); 1.079077875×10^7 km (3); 1.4346705×10^7 km (4);

- 1.790263125 $\times 10^7$ km (5); 2.14585575 $\times 10^7$ km (6);
2.501448375 $\times 10^7$ km (7)
- (ii) Saturnian: r^2 :0.991 Bin delimiters: 0 km (0);
3.644200 $\times 10^6$ km (1); 7.221500 $\times 10^6$ km (2);
1.0798800 $\times 10^7$ km (3); 1.4376100 $\times 10^7$ km (4);
1.7953400 $\times 10^7$ km (5); 2.1530700 $\times 10^7$ km (5)
4. Orbital inclination to the plane(i):
(i) Jovian: r^2 :0.990 Bin delimiters: 0° (0); 16°55 (1);
33°1 (2); 49°65 (3); 66°2 (4); 82°75 (5); 99°3 (6);
115°85 (7); 132°4 (8); 148°95 (9)
(ii) Saturnian: r^2 :0.993 Bin delimiters: 0° (0); 29°97 (1);
59°93 (2); 89°9 (3); 119°87 (4); 149°83 (5)
5. Orbital eccentricity(e):
(i) Jovian: r^2 :0.99 Bin delimiters: 0(0); 0.036 (1); 0.072
(2); 0.108 (3); 0.144 (4); 0.18 (5); 0.216 (6); 0.252 (7);
0.288 (8); 0.324 (9); 0.36 (10); 0.396 (11)
(ii) Saturnian: r^2 :0.993 Bin delimiters: 0 (0); 0.064 (1);
0.129 (2); 0.193 (3); 0.258 (4); 0.322 (5); 0.387 (6);
0.451 (7); 0.515 (8); 0.58 (9)

A.2. Physical Characteristics

1. Density:
(i) Jovian: r^2 :0.996 Bin delimiters: 3084.5 kg m⁻³ (0);
2639 kg m⁻³ (1); 2193.5 kg m⁻³ (2); 1748 kg m⁻³ (3);
1302.5 kg m⁻³ (4); 854.3 kg m⁻³ (5)
(ii) Saturnian: r^2 :0.992 Bin delimiters: 1880 kg m⁻³ (0);
1713.6 kg m⁻³ (1); 1547.3 kg m⁻³ (2); 1380.9 kg m⁻³
(3); 1214.5 kg m⁻³ (4); 1048.2 kg m⁻³ (5); 881.8 kg m⁻³
(6); 715.4 kg m⁻³ (7); 549.1 kg m⁻³ (8); 382.7 kg m⁻³
(9); 216.3 kg m⁻³ (10); 48.2 kg m⁻³ (11)
2. Visual geometric albedo:
(i) Jovian: r^2 :0.991 Bin delimiters: 0 (0); 0.09 (1); 0.16
(2); 0.24 (3); 0.31 (4); 0.38 (5); 0.46 (6); 0.53 (7); 0.60
(8); 0.68 (9)
(ii) Saturnian: r^2 :0.991 Bin delimiters: 0 (0); 0.13 (1);
0.26 (2); 0.38 (3); 0.51 (4); 0.63 (5); 0.75 (6); 0.87 (7)

A.3. Compositional Characteristics

1. Elemental Hydrogen (eH) Presence (0); Absence (1)
2. Hydrogen (H₂) Presence (0); Absence (1)
3. Helium (He) Presence (0); Absence (1)
4. Oxygen (O₂) Absence (0); Presence (1)
5. Ozone (O₃) Absence (0); Presence (1)
6. Sodium (Na) Absence (0); Presence (1)
7. Potassium (K) Absence (0); Presence (1)
8. Carbon dioxide (CO₂) Absence (0); Presence (1)
9. Nitrogen (N₂) Absence (0); Presence (1)
10. Sulphur dioxide (SO₂) Absence (0); Presence (1)
11. Argon (Ar) Absence (0); Presence (1)
12. Water (H₂O) Absence (0); Presence (1)
13. Carbon monoxide (CO) Absence (0); Presence (1)
14. Neon (Ne) Absence (0); Presence (1)
15. Nitrogen oxide (NO) Absence (0); Presence (1)
16. Methane (CH₄) Absence (0); Presence (1)
17. Sulphuric acid (H₂SO₄) Absence (0); Presence (1)
18. Iron (Fe) Absence (0); Presence (1)
19. Nickel (Ni) Absence (0); Presence (1)
20. Iron sulphide (FeS) Absence (0); Presence (1)
21. Iron oxide (FeO) Absence (0); Presence (1)
22. Silicone oxide (SiO) Absence (0); Presence (1)
23. Magnesium oxide (MgO) Absence (0); Presence (1)
24. Basalt (Bas) Absence (0); Presence (1)
25. Sulphur (S) Absence (0); Presence (1)
26. Silicates (Sil) Absence (0); Presence (1)
27. Carbonates (Carb) Absence (0); Presence (1)
28. Ammonia (NH₄) Absence (0); Presence (1)
29. Hydrocarbons (HyCarb) Absence (0); Presence (1)
30. Hydrogen peroxide (H₂O₂) Absence (0); Presence (1)
31. Tholins (Thol) Absence (0); Presence (1)

Appendix B Jovian Satellite Matrix

Here, Table 3 contains the Taxon-character matrix used in the cladistical analysis of the Jovian satellite system.

Table 3
(Continued)

Identifier	Orb	Rev	a	i	e	D	Alb	eH	H ₂	He	O ₂	O ₃	Na	K	CO ₂	N ₂	SO ₂	Ar	H ₂ O	CO	Ne	NO	CH ₄	H ₂ SO ₄	Fe	Ni	FeS	FeO	SiO	MgO	Bas	S	Sil	Carb	NH ₃	HyCarb	H ₂ O ₂	Thol	Reference	
Megaclite	1	1	6.9	11	?	0	1	?	?	?	?	?	?	?	?	?	?	?	?	?	?	?	?	?	?	?	?	?	?	?	?	?	?	?	?	?	?	?	?	16, 17, 18
Sinope	1	1	6.9	6	?	0	1	1	1	0	0	0	0	0	0	0	0	0	0	0	0	0	0	0	0	0	0	0	0	0	0	0	1	1	0	0	0	0	0	16, 17, 18, 19, 21
Hegemone	1	1	6.9	9	?	?	1	?	?	?	?	?	?	?	?	?	?	?	?	?	?	?	?	?	?	?	?	?	?	?	?	?	?	?	?	?	?	?	?	16
Aoede	1	1	6.9	1	?	?	1	?	?	?	?	?	?	?	?	?	?	?	?	?	?	?	?	?	?	?	?	?	?	?	?	?	?	?	?	?	?	?	?	16
Callirrhoe	1	1	6.8	7	?	0	1	1	1	0	0	0	0	0	0	0	0	0	0	0	0	0	0	0	0	0	0	0	0	0	0	0	1	1	0	0	0	0	0	16, 17, 18, 19
Cyllene	1	1	6.9	8	?	?	1	?	?	?	?	?	?	?	?	?	?	?	?	?	?	?	?	?	?	?	?	?	?	?	?	?	?	?	?	?	?	?	?	16
Kore	1	1	6.8	9	?	?	1	?	?	?	?	?	?	?	?	?	?	?	?	?	?	?	?	?	?	?	?	?	?	?	?	?	?	?	?	?	?	?	?	16
S/2003 J2	1	1	7.9	10	?	?	1	?	?	?	?	?	?	?	?	?	?	?	?	?	?	?	?	?	?	?	?	?	?	?	?	?	?	?	?	?	?	?	?	16
S/2003 J3	1	1	5.8	6	?	?	1	?	?	?	?	?	?	?	?	?	?	?	?	?	?	?	?	?	?	?	?	?	?	?	?	?	?	?	?	?	?	?	?	16
S/2003 J4	1	1	6.8	5	?	?	1	?	?	?	?	?	?	?	?	?	?	?	?	?	?	?	?	?	?	?	?	?	?	?	?	?	?	?	?	?	?	?	?	16
S/2003 J5	1	1	6.9	5	?	?	1	?	?	?	?	?	?	?	?	?	?	?	?	?	?	?	?	?	?	?	?	?	?	?	?	?	?	?	?	?	?	?	?	16
S/2003 J9	1	1	6.9	7	?	?	1	?	?	?	?	?	?	?	?	?	?	?	?	?	?	?	?	?	?	?	?	?	?	?	?	?	?	?	?	?	?	?	?	16
S/2003 J10	1	1	6.9	5	?	?	1	?	?	?	?	?	?	?	?	?	?	?	?	?	?	?	?	?	?	?	?	?	?	?	?	?	?	?	?	?	?	?	?	16
S/2003 J12	1	1	5.8	10	?	?	1	?	?	?	?	?	?	?	?	?	?	?	?	?	?	?	?	?	?	?	?	?	?	?	?	?	?	?	?	?	?	?	?	16
S/2003 J15	1	1	6.8	3	?	?	1	?	?	?	?	?	?	?	?	?	?	?	?	?	?	?	?	?	?	?	?	?	?	?	?	?	?	?	?	?	?	?	?	16
S/2003 J16	1	1	5.8	7	?	?	1	?	?	?	?	?	?	?	?	?	?	?	?	?	?	?	?	?	?	?	?	?	?	?	?	?	?	?	?	?	?	?	?	16
S/2003 J18	1	1	5.8	3	?	?	1	?	?	?	?	?	?	?	?	?	?	?	?	?	?	?	?	?	?	?	?	?	?	?	?	?	?	?	?	?	?	?	?	16
S/2003 J19	1	1	6.9	9	?	?	1	?	?	?	?	?	?	?	?	?	?	?	?	?	?	?	?	?	?	?	?	?	?	?	?	?	?	?	?	?	?	?	?	16
S/2003 J23	1	1	6.9	8	?	?	1	?	?	?	?	?	?	?	?	?	?	?	?	?	?	?	?	?	?	?	?	?	?	?	?	?	?	?	?	?	?	?	?	16
S/2010 J1	1	1	6.9	8	?	?	1	?	?	?	?	?	?	?	?	?	?	?	?	?	?	?	?	?	?	?	?	?	?	?	?	?	?	?	?	?	?	?	?	16
S/2010 J2	1	1	5.9	8	?	?	1	?	?	?	?	?	?	?	?	?	?	?	?	?	?	?	?	?	?	?	?	?	?	?	?	?	?	?	?	?	?	?	?	16
S/2011 J1	1	1	5.9	8	?	?	1	?	?	?	?	?	?	?	?	?	?	?	?	?	?	?	?	?	?	?	?	?	?	?	?	?	?	?	?	?	?	?	?	16
S/2011 J2	1	1	6.9	10	?	?	1	?	?	?	?	?	?	?	?	?	?	?	?	?	?	?	?	?	?	?	?	?	?	?	?	?	?	?	?	?	?	?	?	16

Note. Character abbreviations: in orbit around the gas giant (Orb); revolution (Rev); semimajor axis (a); orbital inclination to the plane (i); orbital eccentricity (e); density (D); visual geometric albedo (Alb); elemental hydrogen (eH); hydrogen (H₂); helium (He); oxygen (O₂); ozone (O₃); sodium (Na); potassium (K); carbon dioxide (CO₂); nitrogen (N₂); sulphur dioxide (SO₂); argon (Ar); water (H₂O); carbon monoxide (CO); neon (Ne); nitrogen oxide (NO); methane (CH₄); sulphuric acid (H₂SO₄); iron (Fe); nickel (Ni); iron sulphide (FeS); iron oxide (FeO); silicone oxide (SiO); magnesium oxide (MgO); basalt (Bas); sulphur (S); silicates (Sil); carbonates (Carb); ammonia (NH₃); hydrocarbons (HyCarb); hydrogen peroxide (H₂O₂); and tholins (Thol). The compositional characters eH, H₂, and He have absence indicated by a 1. In the remainder of compositional characteristics, a 1 is indicative of presence of the chemical species.

References. (1) Lodders (2003), (2) Brooks et al. (2004), (3) Brown et al. (2003), (4) Burns et al. (1999), (5) Krüger et al. (2009), (6) Ockert-Bell et al. (1999), (7) Throop et al. (2004), (8) Wong et al. (2006), (9) Thomas et al. (1998), (10) Cooper et al. (2006), (11) Takato et al. (2004), (12) Dalton et al. (2010), (13) Dalton (2010), (14) Greenberg (2010), (15) Hussmann et al. (2006), (16) Beaugé & Nesvorný (2007), (17) Sheppard & Jewitt (2003), (18) Grav et al. (2003), (19) Grav et al. (2015), (20) Rettig et al. (2001), (21) Sykes et al. (2000), (22) Chamberlain & Brown (2004), (23) Emelyanov (2005).

(This table is available in machine-readable form.)

ORCID iDs

Timothy. R. Holt  <https://orcid.org/0000-0003-0437-3296>
 Adrian. J. Brown  <https://orcid.org/0000-0002-9352-6989>
 David Nesvorný  <https://orcid.org/0000-0002-4547-4301>
 Jonathan Horner  <https://orcid.org/0000-0002-1160-7970>
 Brad Carter  <https://orcid.org/0000-0003-0035-8769>

References

- Archie, J. W. 1989, *Systematic Zoology*, 38, 253
 Aria, C., & Caron, J.-B. 2017, *Natur*, 545, 89
 Asphaug, E., & Reufer, A. 2013, *Icar*, 223, 544
 Bakker, R. T., & Galton, P. M. 1974, *Natur*, 248, 168
 Barnard, E. E. 1892, *AJ*, 12, 81
 Baum, W. A., Kreidl, T., Westphal, J. A., et al. 1981, *Icar*, 47, 84
 Beaugé, C., & Nesvorný, D. 2007, *AJ*, 133, 2537
 Blunck, J. 2010, in ASP Conf. Ser. 421, The Satellites of Saturn, ed. L. Verdes-Montenegro, A. del Olmo, & J. Sulentic (Berlin: Springer), 53
 Brandley, M. C., Warren, D. L., Leaché, A. D., & McGuire, J. A. 2009, *Systematic Biol.*, 58, 184
 Brooks, S. M., Esposito, L. W., Showalter, M. R., & Throop, H. B. 2004, *Icar*, 170, 35
 Brown, A. J. 2014, *Icar*, 239, 85
 Brown, R. H., Baines, K. H., Bellucci, G., et al. 2003, *Icar*, 164, 461
 Buratti, B. J., Bauer, J. M., Hicks, M. D., et al. 2010, *Icar*, 206, 524
 Burns, J. A., Showalter, M. R., Hamilton, D. P., et al. 1999, *Sci*, 284, 1146
 Callegari, N., & Yokoyama, T. 2010, in IAU Symp. 263, Icy Bodies of the Solar System, ed. J. A. Fernandez et al. (Cambridge: Cambridge Univ. Press), 161
 Canup, R. M. 2010, *Natur*, 468, 943
 Canup, R. M., & Ward, W. R. 2002, *AJ*, 124, 3404
 Cardone, V. F., & Fraix-Burnet, D. 2013, *MNRAS*, 434, 1930
 Carruba, V., Domingos, R. C., Nesvorný, D., et al. 2013, *MNRAS*, 433, 2075
 Cassini, G. D. 1673, *RSPT*, 8, 5178
 Cassini, G. D. 1686, *RSPT*, 16, 79
 Chamberlain, A., & Wood, B. A. 1987, *J. Hum. Evol.*, 16, 119
 Chamberlain, M. A., & Brown, R. H. 2004, *Icar*, 172, 163
 Charnoz, S., Crida, A., Castillo-Rogez, J. C., et al. 2011, *Icar*, 216, 535
 Charnoz, S., Salmon, J., & Crida, A. 2010, *Natur*, 465, 752
 Christou, A. A. 2005, *Icar*, 174, 215
 Clark, R. N., Brown, R. H., Jaumann, R., et al. 2005, *Natur*, 435, 66
 Clark, R. N., Cruikshank, D. P., Jaumann, R., et al. 2012, *Icar*, 218, 831
 Cobbett, A., Wilkinson, M., Wills, M. A., & Sullivan, J. 2007, *Systematic Biol.*, 56, 753
 Colombo, G., & Franklin, F. A. 1971, *Icar*, 15, 186
 Continuum Analytics 2016, Anaconda Software Distribution, v. 2.4.0, <https://continuum.io>
 Cooper, N. J., Murray, C. D., Porco, C. C., & Spitale, J. N. 2006, *Icar*, 181, 223
 Čuk, M., & Burns, J. A. 2004, *Icar*, 167, 369
 Cuzzi, J. N., Whizin, A. D., Hogan, R. C., et al. 2014, *Icar*, 232, 157
 Dalton, J. B. 2010, *SSRv*, 153, 219
 Dalton, J. B., Cruikshank, D. P., Stephan, K., et al. 2010, *SSRv*, 153, 113
 Darwin, C. 1859, On the Origin of the Species by Natural Selection (London: Murray)
 Deienno, R., Nesvorný, D., Vokrouhlický, D., & Yokoyama, T. 2014, *AJ*, 148, 25
 El Moutamid, M., Nicholson, P. D., French, R. G., et al. 2016, *Icar*, 279, 125
 Emelyanov, N. V. 2005, *A&A*, 438, L33
 Farris, J. S. 1970, *Systematic Biol.*, 19, 83
 Farris, J. S. 1989, *Cladistics*, 5, 417
 Farris, J. S. 1990, *Cladistics*, 6, 91
 Feibelman, W. A. 1967, *Natur*, 214, 793
 Filacchione, G., Capaccioni, F., Ciarniello, M., et al. 2012, *Icar*, 220, 1064
 Filacchione, G., Capaccioni, F., Clark, R. N., et al. 2010, *Icar*, 206, 507
 Filacchione, G., Capaccioni, F., McCord, T. B., et al. 2007, *Icar*, 186, 259
 Filacchione, G., Ciarniello, M., Capaccioni, F., et al. 2014, *Icar*, 241, 45
 Filacchione, G., D'Aversa, E., Capaccioni, F., et al. 2016, *Icar*, 271, 292
 Fraix-Burnet, D., Chattopadhyay, T., Chattopadhyay, A. K., Davoust, E., & Thuillard, M. 2012, *A&A*, 545, A80
 Fraix-Burnet, D., Choler, P., & Douzery, E. J. P. 2006, *A&A*, 455, 845
 Fraix-Burnet, D., & Davoust, E. 2015, *MNRAS*, 450, 3431
 Fraix-Burnet, D., Davoust, E., & Charbonnel, C. 2009, *MNRAS*, 398, 1706
 Fraix-Burnet, D., Dugué, M., Chattopadhyay, T., Chattopadhyay, A. K., & Davoust, E. 2010, *MNRAS*, 407, 2207
 Fraix-Burnet, D., Thuillard, M., & Chattopadhyay, A. K. 2015, *FrASS*, 2, 3
 Galilei, G. 1610, Sidereus Nuncius (Venice: Tommaso Baglioni)
 Gascuel, O. 2005, Mathematics of Evolution and Phylogeny (Oxford: Oxford Univ. Press)
 Giese, B., Neukum, G., Roatsch, T., Denk, T., & Porco, C. C. 2006, *P&SS*, 54, 1156
 Gillon, M., Jehin, E., Lederer, S. M., et al. 2016, *Natur*, 533, 221
 Givnish, T., & Sytsma, K. 1997, *Mol. Phylogenetics Evol.*, 7, 320
 Gladman, B., Kavelaars, J. J., Holman, M., et al. 2001, *Natur*, 412, 163
 Gladman, B., Sheppard, S. S., & Marsden, B. G. 2003a, *IAUC*, 8125
 Gladman, B., Sheppard, S. S., & Marsden, B. G. 2003b, *IAUC*, 8138
 Goloboff, P. A. 1994, *Cladistics*, 9, 433
 Goloboff, P. A. 1996, *Cladistics*, 12, 199
 Goloboff, P. A. 2015, *Cladistics*, 31, 210
 Goloboff, P. A., & Catalano, S. A. 2016, *Cladistics*, 32, 221
 Goloboff, P. A., Farris, J. S., & Nixon, K. C. 2008, *Cladistics*, 24, 774
 Grav, T., & Bauer, J. 2007, *Icar*, 191, 267
 Grav, T., Bauer, J. M., Mainzer, A. K., et al. 2015, *ApJ*, 809, 3
 Grav, T., Holman, M. J., Gladman, B. J., & Aksnes, K. 2003, *Icar*, 166, 33
 Greenberg, R. 2010, *RPPH*, 73, 036801
 Grundy, W. M., Buratti, B. J., Cheng, A. F., et al. 2007, *Sci*, 318, 234
 Hamilton, A. 2014, The Evolution of Phylogenetic Systematics: Species and Systematics Vol. 5 (Berkeley, CA: Univ. California Press)
 Hedman, M. M., Burns, J. A., Hamilton, D. P., & Showalter, M. R. 2012, *Icar*, 217, 322
 Hedman, M. M., Burns, J. A., Showalter, M. R., et al. 2007a, *Icar*, 188, 89
 Hedman, M. M., Burns, J. A., Tiscareno, M. S., et al. 2007b, *Sci*, 317, 653
 Hedman, M. M., Cooper, N. J., Murray, C. D., et al. 2010, *Icar*, 207, 433
 Hedman, M. M., Murray, C. D., Cooper, N. J., et al. 2009, *Icar*, 199, 378
 Hemingway, D., Nimmo, F., Zebker, H., & Jess, L. 2013, *Natur*, 500, 550
 Hennig, W. 1965, *Annu. Rev. Entomology*, 10, 97
 Heppenheimer, T. A., & Porco, C. 1977, *Icar*, 30, 385
 Hillier, J. K., Green, S. F., McBride, N., et al. 2007, *MNRAS*, 377, 1588
 Hirtzig, M., Bézard, B., Lellouch, E., et al. 2013, *Icar*, 226, 470
 Holt, T. R., Brown, A. J., & Nesvorný, D. 2016, *LPSC*, 47, 2676
 Hug, L. A., Baker, B. J., Anantharaman, K., et al. 2016, *Nat. Microbiol.*, 1, 16048
 Hussmann, H., Sohl, F., & Spohn, T. 2006, *Icar*, 185, 258
 Huygens, C. 1659, Systema Saturnium (The Hague: Adriani Vlacq)
 Jacobson, R., Brozovic, M., Gladman, B., et al. 2011, *IAUC*, 9222
 Jewitt, D., & Haghighipour, N. 2007, *ARA&A*, 45, 261
 Jewitt, D., Sheppard, S., Kleyna, J., & Marsden, B. G. 2005, *IAUC*, 8523
 Jewitt, D. C., Danielson, G. E., & Synnott, S. P. 1979, *Sci*, 206, 951
 Jofré, P., Das, P., Bertranpetit, J., & Foley, R. 2017, *MNRAS*, 467, 1140
 Johnson, T. V., & Lunine, J. I. 2005, *Natur*, 435, 69
 Jones, E., Oliphant, T., Peterson, P., et al. 2001, SciPy: Open source scientific tools for Python, <http://www.scipy.org/>
 Karkoschka, E. 1994, *Icar*, 111, 174
 Kluge, A. G., & Farris, J. S. 1969, *Systematic Zoology*, 18, 1
 Korsun, P. P., Rousselot, P., Kulyk, I. V., Afanasiev, V. L., & Ivanova, O. V. 2014, *Icar*, 232, 88
 Kowal, C., Roemer, E., Daniel, M. A., et al. 1975a, *IAUC*, 2855
 Kowal, C. T., Aksnes, K., Marsden, B. G., & Roemer, E. 1975b, *AJ*, 80, 460
 Krüger, H., Hamilton, D. P., Moissl, R., & Grün, E. 2009, *Icar*, 203, 198
 Kuiper, G. P. 1944, *ApJ*, 100, 378
 Lebreton, J.-P., Witasse, O., Sollazzo, C., et al. 2005, *Natur*, 438, 758
 Levison, H. F., Kretke, K. A., & Duncan, M. J. 2015, *Natur*, 524, 322
 Lissauer, J. J. 1987, *Icar*, 69, 249
 Lodders, K. 2003, *ApJ*, 591, 1220
 Lykawka, P. S., & Horner, J. 2010, *MNRAS*, 405, 1375
 Maddison, W. P., Donoghue, M. J., & Maddison, D. R. 1984, *Systematic Biol.*, 33, 83
 Maddison, W. P., & Maddison, D. R. 2015, Zephyr: a Mesquite package for interacting with external phylogeny inference programs, v. 1.1, <https://mesquitezephyr.wikispaces.com>
 Maddison, W. P., & Maddison, D. R. 2017, Mesquite: a modular system for evolutionary analysis, v. 3.20, <http://mesquiteproject.org>
 Margush, T., & McMorris, F. R. 1981, *Bull. Math. Biol.*, 43, 239
 Matson, D. L., Castillo-Rogez, J. C., Schubert, G., Sotin, C., & McKinnon, W. B. 2009, in The Thermal Evolution and Internal Structure of Saturn's Mid-Sized Icy Satellites, ed. M. K. Dougherty, L. W. Esposito, & S. M. Krimigis (Amsterdam: Springer), 577
 McKinney, W. 2010, in Proc. 9th Python in Science Conf. 445, ed. S. van der Walt & J. Millman (Austin, TX: SciPy), 51
 Melotte, J., & Perrine, C. D. 1908, *PASP*, 20, 184
 Milani, A., Cellino, A., Knežević, Z., et al. 2014, *Icar*, 239, 46
 Mitchell, P. C. 1901, *Trans. Linnean Soc.*, 8, 173
 Morbidelli, A., Levison, H. F., Tsiganis, K., & Gomes, R. 2005, *Natur*, 435, 462

- Naylor, G., & Kraus, F. 1995, *Systematic Biol.*, 44, 559
- Nesvorný, D., Alvarelos, J. L. A., Dones, L., & Levison, H. F. 2003, *AJ*, 126, 398
- Nesvorný, D., Beaugé, C., & Dones, L. 2004, *AJ*, 127, 1768
- Nesvorný, D., Bottke, W. F., Jr., Dones, L., & Levison, H. F. 2002, *Natur*, 417, 720
- Nesvorný, D., & Morbidelli, A. 2012, *AJ*, 144, 117
- Nesvorný, D., Vokrouhlický, D., & Deienno, R. 2014, *ApJ*, 784, 22
- Nesvorný, D., Vokrouhlický, D., & Morbidelli, A. 2007, *AJ*, 133, 1962
- Nesvorný, D., Vokrouhlický, D., & Morbidelli, A. 2013, *ApJ*, 768, 45
- Nicholson, P. D., Hamilton, D. P., Matthews, K., & Yoder, C. F. 1992, *Icar*, 100, 464
- Nicholson, P. D., Hedman, M. M., Clark, R. N., et al. 2008, *Icar*, 193, 182
- Nicholson, S. B. 1914, *PASP*, 26, 197
- Nicholson, S. B. 1938, *PASP*, 50, 292
- Nicholson, S. B. 1951, *PASP*, 63, 297
- Niemann, H. B., Atreya, S. K., Bauer, S. J., et al. 2005, *Natur*, 438, 779
- Ockert-Bell, M. E., Burns, J. A., Daubar, I. J., et al. 1999, *Icar*, 138, 188
- Olsen, G. J., Woese, C. R., & Overbeek, R. 1994, *J. Bacteriol.*, 176, 1
- Parker, A., Ivezić, Ž., Jurić, M., et al. 2008, *Icar*, 198, 138
- Perrine, C. D. 1905, *PASP*, 17, 62
- Perrine, C. D., & Aitken, R. G. 1905, *PASP*, 17, 62
- Pickering, E. C. 1899, *ApJ*, 9, 274
- Pickering, W. H. 1905, *AnHar*, 53, 85
- Pollack, J. B., Burns, J. A., & Tauber, M. E. 1979, *Icar*, 37, 587
- Pollack, J. B., Hubickyj, O., Bodenheimer, P., et al. 1996, *Icar*, 124, 62
- Porco, C. C., Baker, E., Barbara, J., et al. 2005, *Sci*, 307, 1226
- Porco, C. C., Helfenstein, P., Thomas, P. C., et al. 2006, *Sci*, 311, 1393
- Porco, C. C., Thomas, P. C., Weiss, J. W., & Richardson, D. C. 2007, *Sci*, 318, 1602
- Rettig, T. W., Walsh, K., & Consolmagno, G. 2001, *Icar*, 154, 313
- Říčan, O., Pialek, L., Almirón, A., & Casciotta, J. 2011, *Zootaxa*, 2982, 1, <http://www.mapress.com/j/zt/article/view/11638>
- Ross, F. E. 1905, *AnHar*, 53, 101
- Salisbury, S. W., Molnar, R. E., Frey, E., & Willis, P. M. 2006, *RSPSB*, 273, 2439
- Salmon, J., & Canup, R. M. 2017, *ApJ*, 836, 109
- Sanderson, M. J., & Donoghue, M. J. 1989, *Evol.*, 43, 1781
- Scotti, J. V., Spahr, T. B., McMillan, R. S., et al. 2000, *IAUC*, 7460
- Sheppard, S. S., Gladman, B., & Marsden, B. G. 2003a, *IAUC*, 8116
- Sheppard, S. S., Gladman, B., & Marsden, B. G. 2004, *IAUC*, 8276
- Sheppard, S. S., Jewitt, D., & Kleyna, J. 2005, *AJ*, 129, 518
- Sheppard, S. S., Jewitt, D., & Kleyna, J. 2006a, *AJ*, 132, 171
- Sheppard, S. S., & Jewitt, D. C. 2003, *Natur*, 423, 261
- Sheppard, S. S., Jewitt, D. C., Fernandez, Y., et al. 2000, *IAUC*, 7525
- Sheppard, S. S., Jewitt, D. C., Fernandez, Y. R., et al. 2001, *IAUC*, 7555
- Sheppard, S. S., Jewitt, D. C., Kleyna, J., et al. 2003b, *IAUC*, 8087
- Sheppard, S. S., Jewitt, D. C., Kleyna, J., & Marsden, B. G. 2006b, *IAUC*, 8727
- Sheppard, S. S., Jewitt, D. C., Kleyna, J., & Marsden, B. G. 2007, *IAUC*, 8836
- Sheppard, S. S., Jewitt, D. C., Kleyna, J., Marsden, B. G., & Jacobson, R. 2002, *IAUC*, 7900
- Sheppard, S. S., & Marsden, B. G. 2003a, *IAUC*, 8088
- Sheppard, S. S., & Marsden, B. G. 2003b, *IAUC*, 8089
- Sheppard, S. S., & Marsden, B. G. 2004, *IAUC*, 8281
- Sheppard, S. S., & Williams, G. V. 2012, *IAUC*, 9252
- Showalter, M. R. 1991, *Natur*, 351, 709
- Smith, B. A., Soderblom, L. A., Johnson, T. V., et al. 1979, *Sci*, 204, 951
- Smith, S. Y., Stockey, R. A., Rothwell, G. W., & Little, S. A. 2017, *J. Systematic Paleontology*, 15, 69
- Spahn, F., Schmidt, J., Albers, N., et al. 2006, *Sci*, 311, 1416
- Sparks, W. B., Hand, K. P., McGrath, M. A., et al. 2016, *ApJ*, 829, 121
- Spencer, J. R., & Nimmo, F. 2013, *AREPS*, 41, 693
- Spitale, J. N., & Tiscareno, M. 2012, in *AAS Meeting*, 44, 414.04
- Spyder Development Team 2015, *Spyder: The Scientific Python Development Environment*, v. 2.3.8, <https://pythonhosted.org/spyder/>
- Suárez-Díaz, E., & Anaya-Muñoz, V. H. 2008, *Stud. Hist. Phil. Sci.*, 39, 451
- Sun, K.-L., Seiß, M., Hedman, M. M., & Spahn, F. 2017, *Icar*, 284, 206
- Sykes, M. V., Nelson, B., Cutri, R. M., et al. 2000, *Icar*, 143, 371
- Synnott, S. P. 1980, *Sci*, 210, 786
- Synnott, S. P. 1981, *Sci*, 212, 1392
- Takato, N., Bus, S. J., Terada, H., Pyo, T.-S., & Kobayashi, N. 2004, *Sci*, 306, 2224
- Tamayo, D., Burns, J. A., Hamilton, D. P., & Hedman, M. M. 2011, *Icar*, 215, 260
- Tamayo, D., Hedman, M. M., & Burns, J. A. 2014, *Icar*, 233, 1
- Thomas, P. C. 2010, *Icar*, 208, 395
- Thomas, P. C., Burns, J. A., Hedman, M., et al. 2013, *Icar*, 226, 999
- Thomas, P. C., Burns, J. A., Rossier, L., et al. 1998, *Icar*, 135, 360
- Throop, H. B., Porco, C. C., West, R. A., et al. 2004, *Icar*, 172, 59
- Tillyard, R. J. 1926, *The Insects of Australia and New Zealand* (Sydney: Angus and Robertson)
- Tiscareno, M. S., Burns, J. A., Hedman, M. M., et al. 2006, *Natur*, 440, 648
- Tosi, F., Turrini, D., Coradini, A., & Filacchione, G. 2010, *MNRAS*, 403, 1113
- Treffenstädt, L. L., Mourão, D. C., & Winter, O. C. 2015, *A&A*, 583, A80
- Tsiganis, K., Gomes, R., Morbidelli, A., & Levison, H. F. 2005, *Natur*, 435, 459
- Turrini, D., Marzari, F., & Beust, H. 2008, *MNRAS*, 391, 1029
- Turrini, D., Marzari, F., & Tosi, F. 2009, *MNRAS*, 392, 455
- Van Dung, V., Giao, P. M., Chinh, N. N., et al. 1993, *Natur*, 363, 443
- Vasundhara, R., Selvakumar, G., & Anbazhagan, P. 2017, *MNRAS*, 468, 501
- Verbiscer, A., French, R., Showalter, M., & Helfenstein, P. 2007, *Sci*, 315, 815
- Verbiscer, A. J., Skrutskie, M. F., & Hamilton, D. P. 2009, *Natur*, 461, 1098
- Winter, O., Souza, A., Sfait, R., et al. 2016, in *AAs Meeting*, 48, 203.03
- Wong, M. H., de Pater, I., Showalter, M. R., et al. 2006, *Icar*, 185, 403
- Yoder, C. F., Colombo, G., Synnott, S. P., & Yoder, K. A. 1983, *Icar*, 53, 431
- Yoder, C. F., Synnott, S. P., & Salo, H. 1989, *AJ*, 98, 1875
- Zappala, V., Cellino, A., Farinella, P., & Knezevic, Z. 1990, *AJ*, 100, 2030
- Zappala, V., Cellino, A., Farinella, P., & Milani, A. 1994, *AJ*, 107, 772
- Zebker, H. A., Marouf, E. A., & Tyler, G. L. 1985, *Icar*, 64, 531
- Zimmermann, W., & Schultz, W. 1931, *Arbeitsweise der botanischen Phylogenetik und anderer Gruppierungswissenschaften* (Munich: Urban & Schwarzenberg)